Biophysical Journal Volume 99 August 2010 1321–1328

Anomalous Diffusion Reports on the Interaction of Misfolded Proteins with the Quality Control Machinery in the Endoplasmic Reticulum

Nina Malchus and Matthias Weiss*
Cellular Biophysics Group, German Cancer Research Center, c/o BIOQUANT, Heidelberg, Germany

ABSTRACT A multitude of transmembrane proteins enters the endoplasmic reticulum (ER) as unfolded polypeptide chains. During their folding process, they interact repetitively with the ER's quality control machinery. Here, we have used fluorescence correlation spectroscopy to probe these interactions for a prototypical transmembrane protein, VSVG ts045, in vivo. While both folded and unfolded VSVG ts045 showed anomalous diffusion, the unfolded protein had a significantly stronger anomaly. This difference subsided when unfolded VSVG ts045 was in a complex with its chaperone calnexin, or when a mutant form of VSVG ts045 with only one glycan was used. Our experimental data and accompanying simulations suggest that the folding sensor of the quality control (UGT1) oligomerizes unfolded VSVG ts045, leading to a more anomalous/obstructed diffusion. In contrast, calnexin dissolves the oligomers, rendering unfolded VSVG ts045 more mobile, and hence prevents poisoning of the ER.

INTRODUCTION

After translation, virtually all transmembrane proteins, i.e., ~30% of the cell's proteome, enter the endoplasmic reticulum (ER) as unfolded polypeptide chains. Here, they undergo chaperone-assisted folding to their tertiary structure (1) and are subsequently packaged into COPII vesicles at distinct ER exit sites (ERES) (2). Homotypic fusion of COPII vesicles beyond the ER yields larger transport intermediates that eventually shuttle nascent proteins toward the juxtanuclear Golgi apparatus (3,4), where the proteins acquire vital posttranslational modifications.

An important and fundamental question in this sequence of events concerns the quality control in the ER, i.e., how do unfolded proteins know that they should reside in the ER rather than entering an emerging COPII vesicle? The mechanism by which this is achieved is still poorly understood and several models have been proposed to explain the phenomenon (5). Based on biochemical data it has been hypothesized that the abundant ER chaperones, e.g., calnexin, build extensive networklike structures in the ER that bind and immobilize unfolded proteins (6). Therefore, unfolded proteins would not be able to enter ERES and hence could not participate in a default anterograde bulk flow. However, the crucial aspect of this model, the immobilization of unfolded proteins, was challenged by the observation that the temperature-sensitive folding mutant VSVG ts045 (sometimes also referred to as tsO-45-G) of the vesicular stomatitis virus G protein was equally mobile on ER membranes in the folded and unfolded state (7). This result, derived via quantitative fluorescence recovery after photobleaching (FRAP) experiments, therefore supported the view of an active cargo selection and concentration into ERES (8).

However, because diffusion on membranes only depends logarithmically on the size of the diffusing entity (9), the available FRAP data did not allow one to draw any conclusion if and to which extent unfolded proteins change their diffusion behavior due to complex formation with the ER's chaperone machinery. Indeed, a change in VSVG ts045's local diffusion properties not only is a signature of an interaction with chaperones but also may have a considerable impact on the frequency and success of interactions with other molecular cofactors (10).

To elucidate the diffusion properties of (un)folded VSVG ts045 and its chaperone calnexin under various conditions, we have utilized fluorescence correlation spectroscopy (FCS) and model simulations of size-dependent obstructed diffusion. Our experimental data clearly show the folding-dependent anomalous diffusion characteristics of VSVG ts045. The significantly stronger anomaly of the unfolded protein most likely reflects a transient oligomerization with the folding sensor UDP-glucose/glycoprotein glucosyl-transferase (UGT1). In contrast, enhancing the association with calnexin yielded a less anomalous diffusion behavior of unfolded VSVG ts045. In addition, mobilizing the abundant translocon complexes of the ER softened the anomaly of unfolded VSVG ts045. Calnexin therefore solubilizes larger clusters of unfolded VSVG ts045 to enhance its diffusion in an obstacle maze of translocons, hence making the unfolded protein more accessible to interactions with other members of the quality control machinery.

MATERIAL AND METHODS

Cell culture

HeLa cells were cultured in Dulbecco's modified Eagle's medium (MEM) supplemented with 10% fetal calf serum, 1% L-glutamine, 1% nonessential

Submitted November 1, 2009, and accepted for publication January 14, 2010.

*Correspondence: m.weiss@dkfz.de

Editor: George Barisas.

0006-3495/10/08/1321/8 $2.00

doi: 10.1016/j.bpj.2010.06.020

amino acids (Invitrogen, Carlsbad, CA), and 1% penicillin and streptomycin. For microscopy, cells were grown on glass coverslips in 12-well dishes or on Lab-Tek chambered coverglass (two-well, thickness No. 1; Nalge Nunc International, Rochester, NY). Transfection with the GFP-tagged ts-O45-G (11) was performed using FuGene 6 (Roche, Basel, Switzerland) and the manufacturer's protocol (0.5 μg DNA, 2 μL FuGene 6 in a total volume of 50 μL supplement-free MEM). The same protocol was used for GFP-tagged GalNAc-T2 (12) and calnexin (13). Cells were incubated for 24 h at the nonpermissive temperature (39.5°C) and then taken to the microscope stage. Here, the temperature was set either to 39.5°C or 32°C. Cells were treated with 1 mM castanospermine (CST), 100 μg/mL cycloheximide (CHX), 100 μM puromycin (PUR), or 5 μg/mL Brefeldin A (BFA) for the indicated times before performing microscopy; the live imaging medium (MEM without phenol red + 25 mM HEPES) also contained the drugs in the respective concentrations.

Microscopy

Imaging and fluorescence correlation spectroscopy (FCS) was performed with a Leica SP2-TCS confocal laser scanning microscope equipped with a water immersion objective (HCX PL APO 63 × 1.2 W CORR) and an FCS-unit (Leica Microsystems, Mannheim, Germany). Samples were illuminated using the 488-nm line of an Argon laser; fluorescence was detected using a bandpass filter (500–530 nm). The pinhole was set to one Airy unit. Microscope and sample were kept at constant temperature by a climate chamber (Life Imaging Services, Basel, Switzerland).

Fluorescence time traces of 20–50 s length were taken for autocorrelation analysis. To reduce the influence of the local ER geometry, we collected FCS data on several loci within the same cell (compare to Fig. 2 *a*) and on a large cell population. We did not observe systematic changes in the FCS curves between different loci and/or cells. FCS data were fitted with the appropriate mathematical expression for diffusion on a two-dimensional substrate (14):

$$C(\tau) = \frac{(1 + f_T \exp(-\tau/\tau_T))/N}{1 + (\tau/\tau_D)^{\alpha}}. \quad (1)$$

Here, α denotes the degree of anomaly of the diffusion while τ_D is the mean dwell time of a particle in the confocal volume (for $\alpha = 1$ this yields the diffusion coefficient via $\tau_D = r_0^2/(4D)$ with the beam waist r_0). The mean number of particles in the confocal volume is denoted by N, whereas f_T denotes the fraction of fluorophores in the triplet state having a lifetime τ_T. For all measurements, $1 < N < 20$. The above expression for $C(\tau)$ can be derived analytically under the assumption that the particles' subdiffusion is described by a Gaussian propagator with a time-dependent diffusion coefficient (14) (see also Supporting Material for details). However, even when the precise stochastic process is a different one, Eq. 1 has been shown to be a good fitting function (15,16) because $C(\tau)$ only relies on the propagator's second moment.

Due to the photophysics of the GFP variant attached to VSVG ts045, the triplet fraction and times were fairly high (17). Still, the diffusive decay could be resolved unambiguously. All measurements were repeated on several days (no systematic variation), and only stable and unambiguous data were taken into account. We also note that a multicomponent approach with different protein sizes and mobilities (e.g., monomers and trimers for VSVG) cannot explain the observed FCS curves as the mobility of the fast pool was higher than that of a lipid (see also discussion in (14)).

Simulations

Monte Carlo simulations for obstructed diffusion were performed using a square lattice (200 × 200 sites, lattice constant $\Delta x = 5$ nm) with periodic boundary conditions. Diffusive steps of 10–20 tracer particles were taken according to the "blind ant" algorithm ($\Delta t = 5$ μs, diffusion coefficient $D_0 = 1$ $\mu m^2/s$). To achieve a subdiffusive behavior, we randomly placed obstacles on 41% of the lattice sites. This value is near to the percolation threshold and thus yields a transient, yet long-lasting subdiffusion with an anomaly $\alpha > 0.7$ (18). Obstacles were allowed to perform a random walk with diffusion constant D_{obst}.

Small tracers (mimicking, for example, protein monomers or dimers) occupied single lattice sites while large tracers (larger oligomers of proteins) occupied a square of four neighboring lattice sites (see Fig. 3 *a*). Due to the logarithmic dependence of the diffusion coefficient on the particle size in two dimensions (9), small and large particles were assumed to move with the same diffusion coefficient D_0. Before monitoring the diffusion for 10^6 time steps, the system was equilibrated for 10^6 time steps. The resulting mean-square displacement (MSD) was fitted with a power law MSD ~ t^{α} to derive the anomaly exponent α. We also validated that the results of these simulations did not depend on the measurement technique, i.e., fitting the MSD yielded the same as the analogous FCS data (see Supporting Material).

RESULTS

Diffusion of VSVG ts045 depends on its folding status

To elucidate the diffusion properties of GFP-tagged VSVG ts045 in the endoplasmic reticulum (ER) of HeLa cells in the folded and unfolded state, we have used fluorescence correlation spectroscopy (FCS) at the permissive and nonpermissive temperatures (32°C and 39.5°C, respectively). At both temperatures, we applied Brefeldin A (BFA), which disrupts the Golgi apparatus and hence, prevented a loss of VSVG ts045 from the ER at the permissive temperature (7). In agreement with previous FRAP experiments (7), we observed that VSVG ts045 is mobile in the ER irrespective of its folding status. Yet, in contrast to the observations via FRAP, which had indicated a similar diffusive mobility for VSVG ts045 in the folded and unfolded state, we found qualitatively and quantitatively different diffusion behaviors in the two states (representative FCS curves are shown in Fig. 1, *a* and *b*).

At both temperatures we observed anomalous instead of normal diffusion when using Eq. 1, i.e., we found a nonlinear growth of the mean-square displacement, MSD ~ t^{α}, with an anomaly exponent $\alpha < 1$ ($\alpha = 1$ for normal diffusion). Trying to fit $C(\tau)$ with an expression for normal diffusion resulted in systematic deviations of the fit curve from the experimental data (see residuals in Fig. 1 *a*). Using a two-component fit with two normally diffusive pools consistently lead to diffusion coefficients of the faster pool that exceeded the mobility of single lipids on model membranes (see also similar discussion in (14)). We therefore relied on the usage of the anomalous diffusion model Eq. 1 that yielded considerably lower residuals (see Fig. 1 *b*).

We observed that the anomaly was significantly stronger for the unfolded VSVG ts045, i.e., α was lower. In the past, subdiffusion has been observed frequently in cells (14,15,19–21) and its emergence reflects on how a protein interacts with its environment (22). To obtain statistically meaningful results, we inspected the distribution of

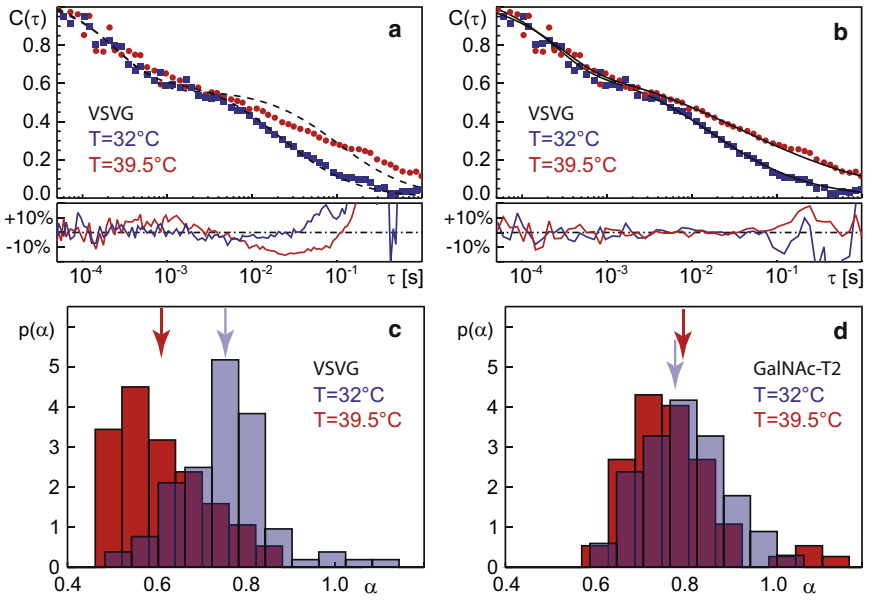

FIGURE 1 (*a*) Representative FCS curves for VSVG ts045 in the ER in the unfolded (*red circles*) and folded (*blue squares*) state at 39.5°C and 32°C, respectively. (*Dashed black lines*) Fits according to Eq. 1 with the constraint $\alpha = 1$, i.e., normal diffusion. The residuals below the autocorrelation functions highlight the systematic deviations of these fits. (*b*) (*Solid black lines*) Fits according to Eq. 1, but with $\alpha < 1$ as an open parameter. The residuals highlight the improved fit to the experimental data. (*c*) The distribution of anomalies, $p(\alpha)$ for VSVG, shows a clear shift from low values in the unfolded state (*red*) toward larger values in the folded state at (*light blue*). (*Arrows*) Mean of the distributions. (*d*) The distributions $p(\alpha)$ for GalNac-T2, a Golgi enzyme that was relocated to the ER by BFA treatment, did not show a significant variation after the temperature shift (*red*, 39.5°C; *light blue*, 32°C)—thereby highlighting the folding-specific behavior of VSVG ts045.

anomalies, $p(\alpha)$, and the associated arithmetic mean, $\langle\alpha\rangle$ in a larger cell population (Fig. 1 *c* and Table 1). In each cell, different loci were used for data acquisition (Fig. 2 *a*) among which no systematic variation of α was detected. We observed that both $p(\alpha)$ and $\langle\alpha\rangle$ showed a significant shift toward smaller α for unfolded VSVG ts045 as compared to the folded form, while the associated mean residence times τ_D did not vary systematically (Table 1). To confirm that the shift in the anomaly was due to folding and not a mere effect of temperature, we performed FCS measurements on GFP-tagged GalNAc-T2 (12), a Golgi-resident transmembrane enzyme that is folded at both temperatures. GalNAc-T2, relocated to the ER via BFA, showed no variation of the anomaly with temperature (Fig. 1 *d*; Table 1). Indeed, GalNAc-T2 showed a statistics $p(\alpha)$ that was similar to the folded VSVG ts045, highlighting a folding-independent background anomaly that may be due to molecular crowding on ER membranes (see Discussion). Thus, the folding of VSVG ts045 rather than the temperature shift itself is responsible for the observed changes in the diffusion behavior.

TABLE 1 Summary of anomalies α and mean residence times τ_D for the indicated proteins at the permissive and nonpermissive temperature for VSVG ts045 folding

		39.5°C	32°C
GalNAc-T2	α	0.80 ± 0.01	0.78 ± 0.02
	τ_D [ms]	9 ± 0.53	13 ± 0.88
	n	56	62
VSVG ts045	α	0.61 ± 0.01	0.75 ± 0.01
	τ_D [ms]	14 ± 0.76	18 ± 0.75
	n	63	87
VSVG ts045 (N336S)	α	0.70 ± 0.02	NA
	τ_D [ms]	43 ± 4.87	NA
	n	33	NA

Testing the significance of the change in α when shifting to 32°C via a Student's *t*-test yielded $p = 0.363$ (GalNAc-T2) and $p = 1.8 \times 10^{-14}$ (VSVG ts045).

Interaction with the ER quality control determines the diffusion anomaly

We next aimed at elucidating the origin of the folding-specific subdiffusion of VSVG ts045. During their interaction with the quality control machinery of the ER, unfolded glycoproteins are known to interact with lectin chaperones like calnexin, glucosidase II (GlcII), and UDP-glucose/glycoprotein glucosyl-transferase (UGT1) via glucose residues on their glycans (1) (see Fig. 2 *b* for a sketch of the folding cycle).

To probe whether the increased anomaly for the unfolded VSVG ts045 was due to the interaction with GlcII, UGT1, or its chaperone calnexin (CNX) (23), we first impaired the folding cycle by blocking the action of GlcII via castanospermine (CST) (6) 1–2 h before performing FCS measurements. Because treatment with CST prevents trimming of the terminal glucose, unfolded VSVG ts045 is well recognized by CNX and is hence not expected to exit the ER even after a shift to the folded state. Indeed, VSVG ts045 was retained in the ER even after shifting to the permissive temperature in the presence of CST (data not shown). However, FCS measurements on the unfolded protein in the presence of CST revealed a significant shift of the anomaly toward the value for folded VSVG ts045 (Table 2) while GalNAc-T2 was not affected at any temperature (data not shown). The latter result is expected because GalNAc-T2 was relocated to the ER in its folded form and hence may not interact with the ER quality control. In addition, we observed a slight increase in the residence time τ_D for VSVG ts045. Hence, only if unfolded VSVG ts045 can interact with GlcII and/or UGT1, is the folding state reflected by the protein's anomalous diffusion behavior.

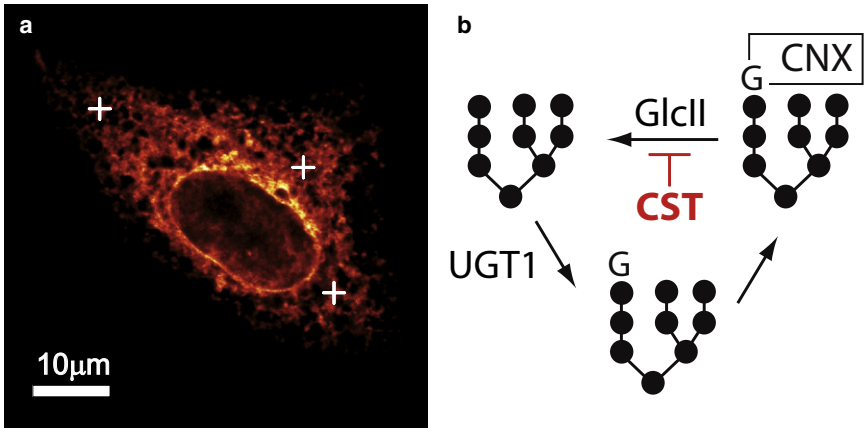

FIGURE 2 (*a*) Representative image of a cell expressing VSVG ts045 at the nonpermissive temperature. (*Open crosses*) Three positions at which FCS experiments have been performed. (*b*) Graphical representation of the biochemically established quality control cycle for VSVG ts045. After trimming of the outermost glucose group by GlcII (which can be inhibited by CST), UGT1 tests the folding state and reglycosylates the glycan of the unfolded protein. The monoglycosylated state is then recognized by CNX. Because UGT1 has been reported to be a dimer, it may induce the formation of transient oligomers of unfolded proteins (see main text for discussion).

To test whether the strong subdiffusion of unfolded VSVG ts045 requires multiple glycans that interact with GlcII and/or UGT1, we utilized the mutant form VSVG ts045(N336S) (24), which lacks one of the two N-glycosylation sites. As a result, VSVG ts045(N336S) showed a significantly less pronounced anomalous diffusion (Table 1) at the nonpermissive temperature, indicating that at least two glycans are needed to induce a strongly anomalous diffusion.

We therefore hypothesized that a dynamic oligomerization of VSVG ts045 with GlcII and/or UGT1 is causal for the folding-specific value of the anomaly.

Abundance of unfolded cargo determines the diffusion properties of calnexin in the ER

To test whether the mobility of CNX is modulated by unfolded proteins, we performed FCS on a GFP-tagged calnexin (13). This approach also allowed us to probe the hypothesis that chaperones form a network that may partially immobilize unfolded proteins in vivo (6). Consistent with earlier reports (24), we observed that calnexin was very mobile in the ER at both temperatures with similar diffusion characteristics (see Table 3), i.e., chaperones are unlikely to form an immobilizing network. The mean anomaly exponent for CNX, however, was lower than that observed for GalNAc-T2 and folded VSVG ts045. A significant increase of α was observed when reducing the amount of newly synthesized (unfolded) cargo by inhibiting protein synthesis via cycloheximide (CHX) (6) 2 h before FCS measurements or when applying CST to avoid complex formation of unfolded proteins with UGT1 (Table 3). This result suggests that CNX (transiently) associates with the subdiffusively moving (putative) oligomers made of unfolded VSVG ts045 and members of the ER quality control.

Obstructed diffusion explains the folding-dependent anomaly

To elaborate on the hypothesis that unfolded VSVG ts045 participates in the formation of larger oligomeric structures, we employed a simulation approach. Although several mechanisms can give rise to anomalous diffusion behavior, the most likely scenario for the case considered here is obstructed diffusion (see Discussion). Previous studies have highlighted that diffusion in a maze of immobile obstacles can lead to anomalous diffusion on extended timescales even if the density of immobile obstacles is not yet at the critical percolation threshold (25). By following this approach, we have tested whether anomalous diffusion can also arise when obstacles are mobile. To this end, we placed obstacles randomly on a two-dimensional square lattice (see Fig. 3 *a*) and allowed tracer particles to move with a diffusive mobility D_0 while obstacles moved with a diffusion coefficient $D_{\text{obst}} \leq D_0$ (see Methods for details). For computational efficiency, we have directly evaluated the particles' MSD, rather than by determining and fitting

TABLE 2 Summary of anomalies α and mean residence times τ_D for VSVG ts045 with the indicated treatment

	39.5°C	32°C	39.5°C + CST	39.5°C + PUR
α	0.61 ± 0.01	0.75 ± 0.01	0.74 ± 0.01	0.74 ± 0.01
τ_D [ms]	14 ± 0.76	18 ± 0.75	30 ± 1.74	30 ± 3.16
n	63	87	56	40

Testing the significance of the anomalies in the respective columns via a Student's t-test yielded $p_{13} = 1.3 \times 10^{-10}$, $p_{23} = 0.489$, $p_{14} = 1.1 \times 10^{-11}$, and $p_{24} = 0.488$. CST, castanospermine; PUR, puromycin.

TABLE 3 Summary of anomalies α and mean residence times τ_D for calnexin (CNX) with the indicated treatment

	39.5°C	32°C	39.5°C + CHX	39.5°C + CST
α	0.68 ± 0.02	0.69 ± 0.02	0.75 ± 0.02	0.73 ± 0.01
τ_D [ms]	28 ± 3.06	27 ± 2.08	21 ± 1.41	47 ± 3.49
n	18	28	18	21

Testing the significance of the anomalies in the respective columns via a Student's t-test yielded $p_{13} = 0.018$, $p_{23} = 0.061$, $p_{14} = 0.021$, and $p_{24} = 0.110$. CHX, cycloheximide; CST, castanospermine.

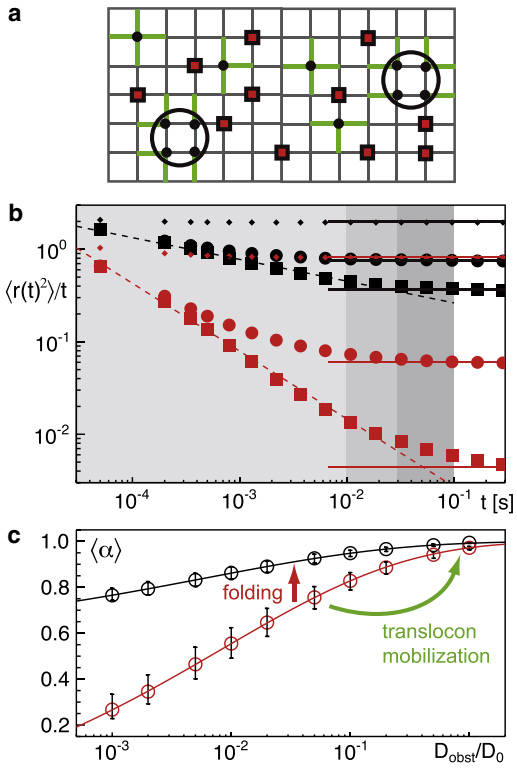

FIGURE 3 (*a*) Setup of the model for obstructed diffusion. Tracer particles (*black circles*) were allowed to move via diffusion (diffusion coefficient D_0) on a square lattice using a Monte Carlo scheme (see Methods). Small tracers occupied single lattice sites while large tracers were taken as tetramers (highlighted by an *enclosing circle*). Obstacles (*red squares*) occupied single lattice sites and were assigned a mobility $D_{obst} \leq D_0$. When a next-neighbor lattice site was blocked, the tracer (or the moving obstacle) was not allowed to hop to this new position whereas hopping to free sites was allowed (highlighted as *green paths*). (*b*) Representative MSDs $\langle r^2(t)\rangle$ as obtained from simulations with small and large tracers (*black* and *red symbols*, respectively). Different mobilities of obstacles: (*small diamonds*) $D_{obst}/D_0 = 1$; (*circles*) $D_{obst}/D_0 = 0.02$; and (*squares*) $D_{obst}/D_0 = 10^{-3}$. (*Dashed lines*) Power-law decays $\langle r^2(t)/t \sim t^{\alpha-1}$ that emerge for $D_{obst}/D_0 << 1$. (*Solid lines*) Asymptotic normal diffusion, $\langle r^2(t)/t = \text{const}$. (*Gray-shaded regions*) Range in which $\langle r^2(t)\rangle \sim t^{\alpha}$ was fitted to extract α. Here, $t < 0.03$ s yielded $\langle\alpha\rangle$, while the ranges $t < 0.01$ s and $t < 0.1$ s were used for determining the uncertainty of $\langle\alpha\rangle$. (*c*) The anomalies $\langle\alpha\rangle$ extracted from $\langle r^2(t)\rangle$ show a strong dependency on the relative mobility of obstacles, D_{obst}/D_0. Upon using a small tracer particle (*black circles*), the anomaly α is enhanced moderately when obstacles become more immobile. Upon using a large tracer (*red circles*), this dependency is much more pronounced. (*Error bars*) Uncertainty associated with the fit range from which α was extracted (see above). Both folding of VSVG ts045 (i.e., making the tracer smaller) and mobilizing obstacles shift α to larger values, in agreement with our experimental data (highlighted by *arrows*).

an FCS autocorrelation function. Both approaches, however, yield the same information (see Supporting Material).

As anticipated, we observed a nonlinear growth of the MSD, $\langle r^2(t)\rangle \sim t^{\alpha}$, with the anomaly α depending on the size of the tracer and the mobility ratio D_{obst}/D_0 (Fig. 3 *b*). A suitable way to highlight the transient nature of the anomalous diffusion below the percolation threshold is a plot of $\langle r^2(t)\rangle/t$, which converges toward a constant for normal diffusion. Indeed, depending on the tracer size and the mobility of the obstacles, the crossover toward the asymptotic normal diffusion occurred earlier or later. As expected, normal diffusion (i.e., $\alpha = 1$) was recovered on all timescales for fully mobile obstacles ($D_{obst}/D_0 \rightarrow 1$). For immobile obstacles ($D_{obst}/D_0 \rightarrow 0$) and small tracers (i.e., tracers and obstacles have the same size), the limiting anomaly $\alpha \approx 0.7$ for two-dimensional percolation (18,25) emerged. In between these extreme cases, the anomaly interpolated itself between the limiting values when fitting the MSD in a reasonable range (highlighted by *gray-shaded regions* in Fig. 3 *b*). The values of α derived from fitting in this range are shown in Fig. 3 *c* as a function of the obstacle mobility, D_{obst}/D_0.

When using larger tracer particles, i.e., a tetramer of small tracers, we observed that the dependency of the anomaly on the ratio D_{obst}/D_0 was considerably enhanced (Fig. 3 *c*): The value of α decreased stronger as compared to small tracers when obstacles became more and more immobile and the apparent anomaly exponents become as low as $\alpha = 0.3$. It is worth noting, however, that the MSD for tetrameric tracer particles is not a clear power law for very low ratios D_{obst}/D_0, but instead, shows a transient kinetic arrest that mimics a power law only on average.

As a result of the simulations, we can state that obstructed diffusion 1), leads to anomalous diffusion even if the obstacles are (slowly) mobile, and 2), that the same obstacle maze yields different anomalies for differently sized protein entities. These findings fit well to our experimental observations if we assume that VSVG ts045 is part of a higher-order structure in its unfolded, but not in its folded form. Whereas unobstructed diffusion in two dimensions only depends logarithmically on the size of the diffusing entity (9) and therefore hardly allows one to determine the oligomeric status, obstacles act as a size-dependent sieve that highlights the oligomeric status. Folded VSVG ts045 proteins (which form homo-trimers (8)) are small entities (= small tracers) that should only feel a minor obstruction of the random walk, i.e., α is large. The unfolded protein, however, interacts repetitively with GlcII and UGT1, the latter of which has been reported to act as a dimer (26). Using the two glycans of VSVG ts045, UGT1 may therefore support oligomer formation of the unfolded protein (= large tracers) with a concomitantly reduced value of α. Shifting to the permissive temperature leads to folding of VSVG ts045, with the diffusing entity becoming smaller because an interaction with UGT1 no longer occurs; consequently, α rises (see Fig. 3 *c*). Alternatively, the oligomeric status can also be broken at the nonpermissive temperature by applying CST (freezing the unfolded protein in a CNX-associated state that does not interact with UGT1) or by deleting one glycan of VSVG ts045 (N336S mutant). In either case, oligomerization of the unfolded protein is hampered, and thus α increases as observed experimentally. Based on this model

we can also predict a new effect: Mobilizing obstacles without affecting the oligomeric status of VSVG ts045 should lead to a softening of the anomaly.

We hypothesized that the highly abundant and fairly immobile translocons, which mediate the translocation of polypeptide chains from ribosomes into the ER, may constitute the diffusion obstacles. Indeed, releasing translocons from ribosomes by applying puromycin (PUR), i.e., enhancing the mobility of translocons (27), we observed a significant shift of the anomaly for unfolded VSVG ts045 while the folded form was not significantly affected (Table 2). These data support our model predictions on a size-dependent anomalous diffusion with translocons acting as (slowly mobile) obstacles that obstruct the diffusion of (un)folded VSVG ts045 according to its effective oligomeric size.

DISCUSSION

We have shown here that the diffusion characteristics of the model cargo VSVG ts045 in ER membranes significantly depends on its folding status. Blocking the interaction with GlcII or using a mutant form with only one glycan resulted in a diffusion behavior of the unfolded protein that was indistinguishable from the folded form. The same reduction of the anomaly was observed when the abundant translocons were mobilized. Together with our model simulations, these data are consistent with the notion that unfolded VSVG ts045 and GlcII or UGT1 form larger complexes that show a strongly obstructed (and hence strongly anomalous) diffusion. Perturbing the formation of oligomers, e.g., by folding of VSVG ts045, adding CST, or using the N336S mutant, yields smaller entities that are less obstructed in their diffusion and thus show a more-normal diffusion behavior. Translocons therefore seem to act as size-selective diffusion obstacles that render the diffusion of unfolded VSVG ts045 more or less anomalous depending on its oligomeric status.

As shown above, two glycans were necessary to obtain a strongly anomalous diffusion, i.e., to induce oligomerization of the unfolded VSVG ts045. Together with the experimental finding that the folding sensor UGT1 acts in a dimeric form (26), this indicates that most likely UGT1, and not GlcII, is responsible for oligomerizing the unfolded VSVG ts045 to larger complexes. After glucose addition to the glycan via UGT1 and the subsequent binding of CNX (see Fig. 2 *b*), the unfolded VSVG ts045 can leave the complex and diffuses on ER membranes as a smaller entity. CNX therefore would be crucial to dissolve larger complexes of unfolded proteins that are tethered dynamically via UGT1. While one could also envisage that unfolded VSVG ts045 irreversibly forms simple aggregates, there is no reason why the N336S mutant with only a single glycan should not show such an aggregation. Moreover, it has been shown that VSVG ts045 is no longer able to leave the ER if it has started forming aggregates (28). Instead, the protein is then targeted to the ER degradation pathway. In our experiments we did observe, however, that VSVG ts045 was capable of reaching the plasma membrane upon shifting to the permissive temperature even after keeping cells at the nonpermissive temperature over night.

Due to the hand-shaking cycle of GlcII, UGT1, and CNX (Fig. 2 *b*), one may expect CNX to also show a more pronounced anomalous diffusion while trying to liberate unfolded proteins from the complex with UGT1. In support of this expectation, we observed that the anomaly of GFP-tagged CNX in untreated cells was significantly lower than that observed for GalNAc-T2 and folded VSVG ts045 (Table 3). A significant increase of α was observed, however, when reducing the amount of newly synthesized (unfolded) cargo.

Inspecting our anomaly exponents, a residual anomaly that is not due to the folding state is apparent. Even for folded VSVG ts045 or GalNAc-T2, we observed $\alpha < 0.8$. We attribute this background anomaly to the highly crowded state of ER membranes with a density of peripheral and transmembrane proteins that may well exceed $5 \times 10^4/\mu m^2$ (29). Indeed, we and others have shown earlier that crowding is intimately connected to anomalous diffusion in intracellular fluids (15,21). However, this anomaly-enhancing effect of crowding was not included in our simulations. As a consequence, $\alpha \rightarrow 1$ for $D_{obst} \rightarrow D_0$ is observed. A more-quantitative comparison of our model and the experimental data would also require us to take the crowding-induced anomaly into account. Still, the relative changes of α in our simplified simulations agree well with those observed in experiments, hence supporting our model.

At first glance, our results seem to be in conflict with previous reports on the diffusion of (un)folded VSVG ts045 obtained via FRAP (7). It is worth noting here, however, that FRAP tests the long-range diffusion of proteins whereas FCS is better suited to monitor the short-range diffusion properties on length- and timescales <1 μm and 100 ms. On these scales, the anomaly α is typically a more robust and meaningful measure for the diffusion properties as compared to the mean residence time τ_D in the FCS focus (see, e.g., (14) for a discussion). Indeed, the values for τ_D showed a fairly wide distribution for each condition which may be explained by the different geometries of the ER membrane that had been in the FCS focus. While these (unknown) geometrical constraints do not impose anomalous diffusion, they can considerably increase the variability of the residence time τ_D (14). Nevertheless, in some cases a significant shift of τ_D emerged, e.g., for the mutant form of VSVG ts045 or when applying CST at the nonpermissive temperature. This slowing-down of the proteins' motion has been observed before (24), yet a molecular reason for it has remained elusive.

Finally, we would like to comment on the choice of the model of obstructed diffusion. While the model prediction

was nicely confirmed by our experiments, one may still wonder whether alternative models could also explain the experimental data reported here. Alternative models are fractional Brownian motion (fBm), in which successive steps are correlated, and a continuous time random walk (CTRW), in which particles take power-law-distributed rests between successive steps. Relating to the latter, it is worth noting that a simple binding event, i.e., a stochastic switching between a bound/slow and a free/fast state with Poissonian statistics, cannot induce anomalous diffusion. The typical binding time of such an event introduces only a single additional timescale into the problem while multiple timescales are needed for the emergence of a subdiffusive scaling of the MSD. These multiple timescales are introduced naturally by fBm, CTRW, or by restricting the diffusion in a self-similar maze of obstacles. Given that we were able to affect the diffusion behavior of VSVG ts045 by applying certain drugs or shifting to the folded state, it appears unlikely that fractional Gaussian noise (the thermal driving force for fBm) is the cause for the experimentally observed anomalous diffusion. Inspecting CTRW as a potential model, we have to note that this process has nonstationary increments and hence shows weak ergodicity breaking. Because we did not observe any aging between successively taken FCS curves and mobilizing potential obstacles (the translocons) that gave experimental support for the obstruction model, we considered a CTRW to be the more unlikely model.

CONCLUSIONS

In this article, we have shown that transmembrane proteins like the model cargo VSVG ts045 show a folding-specific subdiffusion on ER membranes due to the interaction with the folding machinery. Counteracting the associated complex formation, CNX liberates unfolded proteins and dissolves the complexes, hence preventing the formation of immobile structures that potentially could poison the ER.

SUPPORTING MATERIAL

One figure and two equations are available at http://www.biophysj.org/biophysj/supplemental/S0006-3495(10)00732-0.

We thank G. Baldini and I. Wada for sending us the plasmids of the GFP-tagged calnexin and VSVG ts045(S336N) mutants, respectively.

This work was supported by the Institute for Modeling and Simulation in the Biosciences in Heidelberg, Germany. N.M. received funding from The Hartmut Hoffmann-Berling International Graduate School of Molecular and Cellular Biology in Heidelberg, Germany.

REFERENCES

1. Ellgaard, L., and A. Helenius. 2003. Quality control in the endoplasmic reticulum. *Nat. Rev. Mol. Cell Biol.* 4:181–191.
2. Gürkan, C., S. M. Stagg, …, W. E. Balch. 2006. The COPII cage: unifying principles of vesicle coat assembly. *Nat. Rev. Mol. Cell Biol.* 7:727–738.
3. Presley, J. F., N. B. Cole, …, J. Lippincott-Schwartz. 1997. ER-to-Golgi transport visualized in living cells. *Nature.* 389:81–85.
4. Scales, S. J., R. Pepperkok, and T. E. Kreis. 1997. Visualization of ER-to-Golgi transport in living cells reveals a sequential mode of action for COPII and COPI. *Cell.* 90:1137–1148.
5. Hendershot, L. M. 2000. Giving protein traffic the green light. *Nat. Cell Biol.* 2:E105–E106.
6. Tatu, U., and A. Helenius. 1997. Interactions between newly synthesized glycoproteins, calnexin and a network of resident chaperones in the endoplasmic reticulum. *J. Cell Biol.* 136:555–565.
7. Nehls, S., E. L. Snapp, …, J. Lippincott-Schwartz. 2000. Dynamics and retention of misfolded proteins in native ER membranes. *Nat. Cell Biol.* 2:288–295.
8. Balch, W. E., J. M. McCaffery, …, M. G. Farquhar. 1994. Vesicular stomatitis virus glycoprotein is sorted and concentrated during export from the endoplasmic reticulum. *Cell.* 76:841–852.
9. Saffman, P. G., and M. Delbrück. 1975. Brownian motion in biological membranes. *Proc. Natl. Acad. Sci. USA.* 72:3111–3113.
10. Zhou, H. X., G. Rivas, and A. P. Minton. 2008. Macromolecular crowding and confinement: biochemical, biophysical, and potential physiological consequences. *Annu. Rev. Biophys.* 37:375–397.
11. Runz, H., K. Miura, …, R. Pepperkok. 2006. Sterols regulate ER-export dynamics of secretory cargo protein ts-O45-G. *EMBO J.* 25:2953–2965.
12. Röttger, S., J. White, …, T. Nilsson. 1998. Localization of three human polypeptide GalNAc-transferases in HeLa cells suggests initiation of O-linked glycosylation throughout the Golgi apparatus. *J. Cell Sci.* 111:45–60.
13. Granell, S., G. Baldini, …, G. Baldini. 2008. Sequestration of mutated α1-antitrypsin into inclusion bodies is a cell-protective mechanism to maintain endoplasmic reticulum function. *Mol. Biol. Cell.* 19:572–586.
14. Weiss, M., H. Hashimoto, and T. Nilsson. 2003. Anomalous protein diffusion in living cells as seen by fluorescence correlation spectroscopy. *Biophys. J.* 84:4043–4052.
15. Weiss, M., M. Elsner, …, T. Nilsson. 2004. Anomalous subdiffusion is a measure for cytoplasmic crowding in living cells. *Biophys. J.* 87:3518–3524.
16. Szymanski, J., and M. Weiss. 2009. Elucidating the origin of anomalous diffusion in crowded fluids. *Phys. Rev. Lett.* 103:038102.
17. Malchus, N., and M. Weiss. 2010. Elucidating anomalous protein diffusion in living cells with fluorescence correlation spectroscopy—facts and pitfalls. *J. Fluoresc.* 20:19–26.
18. Bouchaud, J. P., and A. Georges. 1990. Anomalous diffusion in disordered media—statistical mechanisms, models and physical applications. *Phys. Rep. Rev. Phys. Lett.* 195:127–293.
19. Wachsmuth, M., W. Waldeck, and J. Langowski. 2000. Anomalous diffusion of fluorescent probes inside living cell nuclei investigated by spatially-resolved fluorescence correlation spectroscopy. *J. Mol. Biol.* 298:677–689.
20. Golding, I., and E. C. Cox. 2006. Physical nature of bacterial cytoplasm. *Phys. Rev. Lett.* 96:098102.
21. Guigas, G., C. Kalla, and M. Weiss. 2007. Probing the nanoscale viscoelasticity of intracellular fluids in living cells. *Biophys. J.* 93:316–323.
22. Metzler, R., and J. Klafter. 2004. The restaurant at the end of the random walk: recent developments in the description of anomalous transport by fractional dynamics. *J. Phys. A.* 37:R161–R208.
23. Hammond, C., and A. Helenius. 1994. Folding of VSV G protein: sequential interaction with BiP and calnexin. *Science.* 266:456–458.
24. Nagaya, H., T. Tamura, …, I. Wada. 2008. Regulated motion of glycoproteins revealed by direct visualization of a single cargo in the endoplasmic reticulum. *J. Cell Biol.* 180:129–143.
25. Saxton, M. J. 1994. Anomalous diffusion due to obstacles: a Monte Carlo study. *Biophys. J.* 66:394–401.

26. Trombetta, S. E., and A. J. Parodi. 1992. Purification to apparent homogeneity and partial characterization of rat liver UDP-glucose: glycoprotein glucosyltransferase. *J. Biol. Chem.* 267:9236–9240.

27. Nikonov, A. V., E. Snapp, …, G. Kreibich. 2002. Active translocon complexes labeled with GFP-Dad1 diffuse slowly as large polysome arrays in the endoplasmic reticulum. *J. Cell Biol.* 158:497–506.

28. Molinari, M., C. Galli, …, R. J. Kaufman. 2005. Persistent glycoprotein misfolding activates the glucosidase II/UGT1-driven calnexin cycle to delay aggregation and loss of folding competence. *Mol. Cell.* 20:503–512.

29. Quinn, P., G. Griffiths, and G. Warren. 1984. Density of newly synthesized plasma membrane proteins in intracellular membranes. II. Biochemical studies. *J. Cell Biol.* 98:2142–2147.